



Published in final edited form as:

Dev Biol. 2016 September 1; 417(1): 4–10. doi:10.1016/j.ydbio.2016.07.001.

A novel ciliopathic skull defect arising from excess neural crest

Jacqueline M. Tabler¹, Christopher P. Rice¹, Karen J. Liu^{2,*}, and John Wallingford^{1,*}

Karen J. Liu: karen.liu@kcl.ac.uk; John Wallingford: Wallingford@austin.utexas.edu

¹Department of Molecular Biosciences, University of Texas at Austin

²Department of Craniofacial Development and Stem Cell Biology, King's College London

Abstract

The skull is essential for protecting the brain from damage, and birth defects involving disorganization of skull bones are common. However, the developmental trajectories and molecular etiologies by which many craniofacial phenotypes arise remain poorly understood. Here, we report a novel skull defect in ciliopathic Fuz mutant mice in which only a single bone pair encases the forebrain, instead of the usual paired frontal and parietal bones. Through genetic lineage analysis, we show that this defect stems from a massive expansion of the neural crest-derived frontal bone. This expansion occurs at the expense of the mesodermally-derived parietal bones, which are either severely reduced or absent. A similar, though less severe, phenotype was observed in Gli3 mutant mice, consistent with a role for Gli3 in cilia-mediated signaling. Excess crest has also been shown to drive defective palate morphogenesis in ciliopathic mice, and that defect is ameliorated by reduction of fgf8 gene dosage. Strikingly, skull defects in Fuz mutant mice are also rescued by loss of one allele of fgf8, suggesting a potential route to therapy. In sum, this work is significant for revealing a novel skull defect with a previously un-described developmental etiology and for suggesting a common developmental origin for skull and palate defects in ciliopathies.

Keywords

Cilia; ciliopathy; Fuz; Fgf8; neural crest; craniofacial; skull; calvaria; coronal suture; Greig cephalopolysyndactyly; morphogenesis; craniosynostosis; Wnt1; Mesp1; mouse

Introduction

Craniofacial defects are among the most common and varied human congenital anomalies, affecting at least 1 in 600 live births (Mossey, 2003). While some classes of skull defect are increasingly well understood, there are many for which the etiology remains largely unknown, and even unexplored. For example, the most common skull vault defect has been

*Corresponding author: Karen J. Liu. King's College London, Dept of Craniofacial. Development & Stem Cell Biology. Floor 27, Tower Wing. London, UK SE1 9RT. Tel: +44 20 7188 8035. *Corresponding author: John B. Wallingford. University of Texas, Dept. of Molecular Biosciences. Patterson Labs. 2401 Speedway. Austin, Tx. 78712. Tel: +44512-232-2784.

Publisher's Disclaimer: This is a PDF file of an unedited manuscript that has been accepted for publication. As a service to our customers we are providing this early version of the manuscript. The manuscript will undergo copyediting, typesetting, and review of the resulting proof before it is published in its final citable form. Please note that during the production process errors may be discovered which could affect the content, and all legal disclaimers that apply to the journal pertain.

comprehensively studied: Craniosynostosis is a premature fusion of the cranial sutures for which several causative genes are known and for which mouse models are available (Mossey, 2003, Twigg and Wilkie, 2015, Johnson and Wilkie, 2011). By contrast, craniofacial phenotypes such as acalvaria, calvarial thinning and collapsed calvaria remain only very poorly understood as a result of the paucity of human genetic studies and/or mouse models (Moore et al., 1999, Tokumaru et al., 1996). A deeper etiological understanding of the full spectrum of skull defects is an important challenge for developmental biologists, and could inform individual treatment paradigms and comfort both patients and their families.

This diversity in human skull anomalies reflects the complexity of mammalian skull morphogenesis. For example, two of the major bone pairs in the neurocranium, the frontal and parietal bones, are derived from different embryonic lineages. Both of these bones are required to protect the forebrain, and while the frontal bones are neural crest-derived, parietal bones arise from paraxial mesoderm (Jiang et al., 2002, Yoshida et al., 2008). Previous lineage analyses have shown that neural crest- and mesoderm-derived skull mesenchyme maintain their boundary at the coronal suture until birth (Merrill et al., 2006, Yoshida et al., 2008, Jiang et al., 2002). In addition to maintaining lineage boundaries, the initial positioning of neural crest- and mesoderm-derived mesenchyme must also be tightly regulated relative to the underlying brain. Initially, the entire forebrain is encased by neural crest, however, the caudal half later is covered by mesoderm (Jiang et al., 2002, Yoshida et al., 2008) (see Fig. S1). As such, the border between neural crest- and mesoderm-derived skull mesenchyme must reposition during cranial morphogenesis. Strikingly, however, the developmental time window in which such repositioning occurs has not been characterized.

Here, we report a novel skull phenotype in a ciliopathic mutant mouse. We show that only a single calvarial bone plate encases the forebrain in mice lacking *Fuz*, an essential regulator of ciliogenesis (Park et al., 2006, Gray et al., 2009). To elucidate the etiology of this defect, we characterized early morphogenesis of the frontal and parietal bones. We find that *Fuz* mutants develop a novel skull phenotype in which the neural crest-derived frontal mesenchyme is enlarged at the expense of the parietal mesenchyme, and thus mutants develop only a single calvarial bone pair. We previously showed that *Gli3* processing was disrupted in *Fuz* mutant mice, and accordingly, we now show that neural crest-derived frontal mesenchyme is also expanded in *Gli3^{xt-j/x-jt}* mutant mice at the expense of the parietal bone. Finally, parietal bone formation was rescued when *Fgf8* was genetically reduced in *Fuz* mutants, suggesting that expansion of *Fgf8* in *Fuz* mice is responsible for increased frontal mesenchyme. These findings provide new insights into pathological skull development generally, and potentially shed light on ciliopathies, *Gli3*-related Grieg Cephalopolysyndactyly and FGF-related craniofacial syndromes.

Results and Discussion

Only a single calvarial bone pair develops in *Fuz* mutant mice

Previously, we reported that no coronal suture was evident at E17.5 in *Fuz* mutant mice (Tabler et al., 2013, Yannakoudakis and Liu, 2013). Such absence of a coronal suture has generally been attributed to coronal craniosynostosis –or premature fusion- of frontal and

parietal bone pairs (Johnson and Wilkie, 2011). To our surprise, however, our analysis of the developmental trajectory of frontal and parietal bone mesenchyme in Fuz mutant mice revealed an entirely distinct etiology. Rather than premature fusion of a patent suture separating two bone pairs, Fuz mutant mice actually display only a single bone pair, even at the very earliest stages of skull development. For example, alizarin red staining revealed only a single calvarial bone pair in E15.5 Fuz mutants, though two bones were apparent in littermate controls (Fig. 1A, B). A single bone pair was also observed at E13.5, the very onset of skull mineralization (Fig. 1D). Because coronal craniosynostosis in mouse models occurs from fusion of bones at E14.5 (Chen et al., 2014, Merrill et al., 2006, Yoshida et al., 2005, Holmes et al., 2009), the presence of only a single bone pair a full day earlier suggested that the skull defect in Fuz mutants may represent a novel phenotype involving a failure in the initial formation of two bone pairs that overly the forebrain.

To test this idea, we observed the developing osteogenic condensations of the skull bones prior to mineralization. We examined the calvaria of normal and Fuz mutant mice using a reporter mouse in which GFP is expressed in calvarial condensations at E12.5 under the control of the *Osx1* promoter (Nakashima et al., 2002, Rodda and McMahon, 2006, Strecker et al., 2013). Horizontal sections of *Osx1*-GFP::Cre control mice revealed two distinct calvarial *Osx1* expression domains in WT embryos (Fig. 1F–F'), consistent with the normal patterning of frontal and parietal bone pairs. In contrast, we consistently observed only a single *Osx1*-positive domain in Fuz mutants; no *Osx1*-negative region (i.e. no intervening suture) was observed (Fig. 1G–G', compared to F–F', see also Fig. S1). Thus, only a single bone pair was present in Fuz mutants at all stages examined, from the very onset of terminal osteoblast differentiation at E12.5 to differentiated bone at E17.5.

The single calvarial bone pair in Fuz mutant mice is neural crest-derived

The frontal and parietal bone pairs have distinct developmental origins, with the frontal bone arising from the neural crest and the parietal from mesoderm (Yoshida et al., 2008, Jiang et al., 2002). The single mineralization site we observed in Fuz mutants was positioned apical to the eye, so we reasoned that the single calvarial bone in these mice may be analogous to the frontal bone in normal embryos. To test this idea, we tracked neural crest derived cells in Fuz mutants using *Wnt1*Cre driving GFP (Danielian et al., 1998, Muzumdar et al., 2007). In control embryos at E13.5, neural crest contributed to the thick frontal bone mesenchyme covering the rostral half of the brain, as well as the thin layer of meninges wrapping the entire forebrain (Fig. 2B), consistent with previous reports (Gagan et al., 2007, Jiang et al., 2002, Nagy, 2003). By contrast, neural crest mesenchyme was expanded caudally in Fuz mutants; a thick layer of labeled cells was observed covering the entire forebrain (Fig. 3C, see also S2), suggesting that the single, large calvarial condensation in Fuz mutants comprises expanded frontal bone mesenchyme (Fig. 2C, C'). Indeed, *Osx1* positive cells were only observed in the neural crest derived mesenchyme of Fuz mutants at E14.5 (Fig. 2H, I). Additionally, we measured the thickness of the ectomesenchyme that gives rise to the neural crest derived frontal bone and found a significant increase in ectomesenchymal thickness at E13.5. Moreover, we found an increase in the number of *Twist1* positive ectomesenchymal cells in Fuz mutants (Fig. S2). Taken together these data are consistent

with our previous findings demonstrating that Fuz mutants generate an excess of cranial neural crest at E9.0 (Tabler et al 2013).

The frontal/parietal boundary repositions relative to the brain during normal skull morphogenesis but fails to reposition in Fuz mutants

Our data demonstrate that only a single, enlarged calvarial bone pair forms in Fuz mutant mice. Because this single bone pair is crest-derived, it likely represents an expanded frontal bone. Parietal bones and coronal sutures are both derived from paraxial mesoderm (Deckelbaum et al., 2012, Yoshida et al., 2008). Therefore, an important question arising from these data regards the fate of the cranial paraxial mesoderm that gives rise to parietal bones and coronal sutures in Fuz mutants. We therefore used *Mesp1*Cre driver to lineage trace (Yoshida et al., 2008) morphogenesis of the mesoderm-derived mesenchyme that gives rise to parietal bones in normal mice and in Fuz mutants.

At E11.5, prior to calvarial osteoblast differentiation, labeled paraxial mesoderm in normal mice is observed caudal to the forebrain (Fig. 2F). By E12.5, however, the forebrain lobes have expanded such that labeled mesoderm now forms a wedge of cells overlapping the caudal edge of the cortex (Fig. 2G). By E13.5, mesodermal cells overlap the entire caudal half of the cortex (Fig. 2H). Interestingly, we noted that the normal boundary between neural crest- and mesoderm-derived mesenchyme is positioned roughly at the level of the forebrain-midbrain flexure at all stages analyzed (FB-MB boundary, Fig. 2B–H, see also Fig. S3). Using this flexure as a landmark, our data suggest that mesoderm-derived parietal mesenchyme may not actively move to their final position. Rather, the forebrain appears to expand, filling in underneath the parietal mesenchyme, such that parietal morphogenesis occurs passively.

In striking contrast to normal mice, *Mesp1*-cre driven lineage labeling of Fuz mutants revealed that paraxial mesoderm never overlapped the forebrain, remaining instead in a caudal position over the midbrain (Fig. 2C–C'). Coupled to the absence of detectable ossified parietal bones at later stages, these data raise the possibility that the normal morphogenetic events that juxtapose parietal bone and coronal suture mesenchyme with the cortex may be essential for the transmission of inductive signals from underlying dura mater that drive parietal ossification (Gagan et al., 2007, Li et al., 2007, Spector et al., 2002a, Spector et al., 2002b, Deckelbaum et al., 2012), a possibility that is of interest because frontal and parietal bones are known to respond differently to a variety of osteogenic factors (Li et al., 2010, Quarto et al., 2010). Together with our *Wnt1*-cre lineage analyses, these results suggest that the enlarged neural crest-derived frontal bone forms at the expense of the mesoderm-derived parietal bone in Fuz mutant mice. The positioning of *Mesp1*-cre labeled parietal mesenchyme in E13.5 Fuz mutants is comparable to the positioning of labeled parietal mesenchyme in E11.5 WT embryos (Figure S3). We tested whether a reduction in proliferation or an increase in cell death prohibits parietal mesenchyme from overlapping the forebrain. However we found no change in proliferation or cell death in parietal mesenchyme of mutant embryos at E11.5 (Figure S4) or E12.5 (data not shown). These data suggest that the single bone pair observed in Fuz mutants is not caused by reduced parietal

mesenchyme, further supporting our hypothesis that lack of mesoderm-derived parietal bone in mutants is the result of increased neural crest.

Gli3 loss also elicits expansion of frontal mesenchyme at the expense of parietal mesenchyme

Cilia are essential for Gli-mediated Hedgehog signaling (Huangfu and Anderson, 2006, Huangfu and Anderson, 2005), and Fuz mutant mice display defects in processing of Gli3 (Tabler et al., 2013, Heydeck et al., 2009). To better understand the molecular basis of the novel skull defects in Fuz mutant mice, we examined skull development in Gli3^{xt-j} mutant mice (Hui and Joyner, 1993). Using Wnt1-Cre to drive GFP expression, we found that while coronal sutures were evident, the neural crest-derived frontal bone mesenchyme was substantially expanded in Gli3 mutants at E13.5 compared to controls (Fig 3 C', compared to B). Moreover, we observed a significant reduction in parietal mesenchyme overlapping the forebrain in Wnt1-Cre::GFP labeled Gli3 mutants (Fig C' C'). Though less severe, these findings reflected the frontal expansion observed in Fuz mice. Finally, we asked whether the reduced parietal bone mesenchyme at early stages was related to overt skeletal defects at later stages. We measured parietal bone length using Alizarin red staining at E17.5, and indeed, we observed a significant reduction in parietal bone length in horizontal sections. These data are significant both for providing genetic evidence that reduced Gli3 repressor function underlies Fuz mutant cranial defects and for demonstrating that excess neural crest is a common feature of skull defects both in Fuz and Gli3 mutant mice.

The skull defect in Fuz mutants is ameliorated by reduction of Fgf8 gene dosage

Our lineage tracing data suggest that the single bone pair in mutants results from an excess of neural crest-derived skull mesenchyme (Fig. 3C) and neural specific Fgf8 expression is crucial for maintaining cranial neural crest cell numbers (Fish et al., 2014, Tabler et al., 2013, Creuzet et al., 2005). We therefore asked whether reducing Fgf8 may also rescue the defective skull morphology in Fuz mutants. Strikingly, skeletal preps revealed that the skull phenotype described above (Fig. 1) was entirely ameliorated in Fuz mutants that also carried a heterozygous LacZ knockin allele at the Fgf8 locus (Fuz^{-/-}; Fgf8^{lacz/+}) (Ilagan et al., 2006) (Fig. 4B). Frontal and parietal bones were separated by an unossified coronal suture in these mice, as they were in mice lacking the Fuz mutation (Fuz^{+/+}; Fgf8^{lacz/+}) (Fig. 4A). Thus, loss of a single Fgf8 allele was sufficient to rescue a constellation of craniofacial phenotypes spanning the skull (this study), the eye (Fig. 1) and the palate (Tabler et al., 2013) in a ciliopathy mouse model.

Our data argue that an excess of cranial neural crest is a key factor in the etiology of skull defects in the Fuz mutant mice. Together with our previous finding that excess neural crest also contributes to the palate defect in these mice (Tabler et al., 2013), our new data argue that excess crest may be a unifying factor for cranial and facial phenotypes in ciliopathic mice.

In conclusion, data here chart the developmental trajectory of a novel skull defect in a ciliopathic mouse model. While this defect appears superficially similar to craniosynostosis at later stages, a more careful analysis across developmental time revealed that only a single

neural crest-derived bone ever developed in Fuz mutants. Strikingly, this expansion of the frontal bone occurred at the expense of the mesoderm-derived parietal bone. This work thus adds defective parietal morphogenesis to the spectrum of cranial vault anomalies that include not only craniosynostosis, but acalvaria and collapsed calvaria (Moore et al., 1999, Tokumaru et al., 1996). A reduction in parietal bone length was also observed in Gli3 mutant mice and was ameliorated by reduction of Fgf8 gene dosage in Fuz mutants, so these data may also shed light on Gli-related syndromes such as Greig Cephalopolysyndactyly (Panigrahi, 2011, Kwee and Lindhout, 1983), and FGF-related syndromes such as Aperts and Crouzon (Yannakoudakis and Liu, 2013). Finally, this work illustrates the power of embryological and genetic approaches in defining subtle yet critical morphogenetic events that may underlie pathogenic cranial development.

Materials and Methods

Mouse lines

The following mouse lines were used. Fuz mutants: Fuz^{gt(neo)} (Gray et al., 2009), Fgf8 mutants: Fgf8^{lacZ} (Ilagan et al., 2006), Gli3 mutants: Gli3^{xt-j} (Hui and Joyner, 1993), Wnt1-cre driver: Tg(Wnt1-cre)11Rth (Danielian et al., 1998), Mesp1-cre driver: (Saga et al., 1999) and reporter lines: R26R^{mT/mG}: GT(Rosa)26Sor^{tm4}(ACTB-tdTomato-EGFP)^{Luo} (Muzumdar et al., 2007) and Osx1-GFP::Cre: Tg(Sp7-tTA,tetO-EGFP/cre)1Amc (Rodda and McMahon, 2006). Genotyping was performed as described in original publications.

Histology

All immunohistochemistry, and histological staining were performed according to standard protocols. Twist immunohistochemistry was performed using anti-Twist1a (ab50887, Abcam). 12µm cryosections were obtained from embryos fixed overnight in 4%PFA. Images of sections were tiled z-stacks obtained using the Zeiss 700 confocal microscope and Plan-Aprochromat 40x/1.0 objective. Images were presented as maximum projections from 10µm confocal z-stacks where the optical slice size was 1.2µm. Alizarin red staining was performed according to (Nagy, 2003). Wholemout images were obtained using the Zeiss AXIO zoom V16.

Supplementary Material

Refer to Web version on PubMed Central for supplementary material.

Acknowledgments

We thank Basil Yannakoudakis and Hadeel Adel Al-lami for generating mice in the Liu Lab, and Mitch Butler for critical reading of the manuscript. J.M.T. is supported by a National Research Service Award from the NIDCR F32DE023272. This work was supported by funding from the BBSRC (BB/I021922/1) to K.J.L., a Wellcome Trust Value in People Award to K.J.L. and J.M.T., and by grants from the NIGMS and the NHLBI to J.B.W. J.B.W. is an Early Career Scientist of the HHMI.

References

CHEN P, ZHANG L, WENG T, ZHANG S, SUN S, CHANG M, LI Y, ZHANG B, ZHANG L. A Ser252Trp mutation in fibroblast growth factor receptor 2 (FGFR2) mimicking human Apert

- syndrome reveals an essential role for FGF signaling in the regulation of endochondral bone formation. *PLoS One*. 2014; 9:e87311. [PubMed: 24489893]
- CREUZET S, COULY G, LE DOUARIN NM. Patterning the neural crest derivatives during development of the vertebrate head: insights from avian studies. *J Anat*. 2005; 207:447–59. [PubMed: 16313387]
- DANIELIAN PS, MUCCINO D, ROWITCH DH, MICHAEL SK, MCMAHON AP. Modification of gene activity in mouse embryos in utero by a tamoxifen-inducible form of Cre recombinase. *Curr Biol*. 1998; 8:1323–6. [PubMed: 9843687]
- DECKELBAUM RA, HOLMES G, ZHAO Z, TONG C, BASILICO C, LOOMIS CA. Regulation of cranial morphogenesis and cell fate at the neural crest-mesoderm boundary by engrailed 1. *Development*. 2012; 139:1346–58. [PubMed: 22395741]
- FISH JL, SKLAR RS, WORONOWICZ KC, SCHNEIDER RA. Multiple developmental mechanisms regulate species-specific jaw size. *Development*. 2014; 141:674–84. [PubMed: 24449843]
- GAGAN JR, THOLPADY SS, OGLE RC. Cellular dynamics and tissue interactions of the dura mater during head development. *Birth Defects Res C Embryo Today*. 2007; 81:297–304. [PubMed: 18228258]
- GRAY RS, ABITUA PB, WLODARCZYK BJ, SZABO-ROGERS HL, BLANCHARD O, LEE I, WEISS GS, LIU KJ, MARCOTTE EM, WALLINGFORD JB, FINNELL RH. The planar cell polarity effector Fuz is essential for targeted membrane trafficking, ciliogenesis and mouse embryonic development. *Nat Cell Biol*. 2009; 11:1225–32. [PubMed: 19767740]
- HEYDECK W, ZENG H, LIU A. Planar cell polarity effector gene Fuzzy regulates cilia formation and Hedgehog signal transduction in mouse. *Dev Dyn*. 2009; 238:3035–42. [PubMed: 19877275]
- HOLMES G, ROTHSCILD G, ROY UB, DENG CX, MANSUKHANI A, BASILICO C. Early onset of craniosynostosis in an Apert mouse model reveals critical features of this pathology. *Dev Biol*. 2009; 328:273–84. [PubMed: 19389359]
- HUANGFU D, ANDERSON KV. Cilia and Hedgehog responsiveness in the mouse. *Proc Natl Acad Sci U S A*. 2005; 102:11325–30. [PubMed: 16061793]
- HUANGFU D, ANDERSON KV. Signaling from Smo to Ci/Gli: conservation and divergence of Hedgehog pathways from *Drosophila* to vertebrates. *Development*. 2006; 133:3–14. [PubMed: 16339192]
- HUI CC, JOYNER AL. A mouse model of greig cephalopolysyndactyly syndrome: the extra-toesJ mutation contains an intragenic deletion of the Gli3 gene. *Nat Genet*. 1993; 3:241–6. [PubMed: 8387379]
- ILAGAN R, ABU-ISSA R, BROWN D, YANG YP, JIAO K, SCHWARTZ RJ, KLINGENSMITH J, MEYERS EN. Fgf8 is required for anterior heart field development. *Development*. 2006; 133:2435–45. [PubMed: 16720880]
- JIANG X, ISEKI S, MAXSON RE, SUICOV HM, MORRIS-KAY GM. Tissue origins and interactions in the mammalian skull vault. *Dev Biol*. 2002; 241:106–16. [PubMed: 11784098]
- JOHNSON D, WILKIE AO. Craniosynostosis. *Eur J Hum Genet*. 2011; 19:369–76. [PubMed: 21248745]
- KWEE ML, LINDHOUT D. Frontonasal dysplasia, coronal craniosynostosis, pre- and postaxial polydactyly and split nails: a new autosomal dominant mutant with reduced penetrance and variable expression? *Clin Genet*. 1983; 24:200–5. [PubMed: 6627724]
- LI S, QUARTO N, LONGAKER MT. Dura mater-derived FGF-2 mediates mitogenic signaling in calvarial osteoblasts. *Am J Physiol Cell Physiol*. 2007; 293:C1834–42. [PubMed: 17913846]
- LI S, QUARTO N, LONGAKER MT. Activation of FGF signaling mediates proliferative and osteogenic differences between neural crest derived frontal and mesoderm parietal derived bone. *PLoS One*. 2010; 5:e14033. [PubMed: 21124973]
- MERRILL AE, BOCHUKOVA EG, BRUGGER SM, ISHII M, PILZ DT, WALL SA, LYONS KM, WILKIE AO, MAXSON RE JR. Cell mixing at a neural crest-mesoderm boundary and deficient ephrin-Eph signaling in the pathogenesis of craniosynostosis. *Hum Mol Genet*. 2006; 15:1319–28. [PubMed: 16540516]

- MOORE K, KAPUR RP, SIEBERT JR, ATKINSON W, WINTER T. Acalvaria and hydrocephalus: a case report and discussion of the literature. *J Ultrasound Med.* 1999; 18:783–7. [PubMed: 10547112]
- MOSSEY P. Global strategies to reduce the healthcare burden of craniofacial anomalies. *Br Dent J.* 2003; 195:613. [PubMed: 14631452]
- MUZUMDAR MD, TASIC B, MIYAMICHI K, LI L, LUO L. A global double-fluorescent Cre reporter mouse. *Genesis.* 2007; 45:593–605. [PubMed: 17868096]
- NAGY, A. *Manipulating the mouse embryo: a laboratory manual.* Cold Spring Harbor, N.Y: Cold Spring Harbor Laboratory Press; 2003.
- NAKASHIMA K, ZHOU X, KUNKEL G, ZHANG Z, DENG JM, BEHRINGER RR, DE CROMBRUGGHE B. The novel zinc finger-containing transcription factor osterix is required for osteoblast differentiation and bone formation. *Cell.* 2002; 108:17–29. [PubMed: 11792318]
- PANIGRAHI I. Craniosynostosis genetics: The mystery unfolds. *Indian J Hum Genet.* 2011; 17:48–53. [PubMed: 22090712]
- PARK TJ, HAIGO SL, WALLINGFORD JB. Ciliogenesis defects in embryos lacking inturned or fuzzy function are associated with failure of planar cell polarity and Hedgehog signaling. *Nat Genet.* 2006; 38:303–11. [PubMed: 16493421]
- QUARTO N, WAN DC, KWAN MD, PANETTA NJ, LI S, LONGAKER MT. Origin matters: differences in embryonic tissue origin and Wnt signaling determine the osteogenic potential and healing capacity of frontal and parietal calvarial bones. *J Bone Miner Res.* 2010; 25:1680–94. [PubMed: 19929441]
- RODDA SJ, MCMAHON AP. Distinct roles for Hedgehog and canonical Wnt signaling in specification, differentiation and maintenance of osteoblast progenitors. *Development.* 2006; 133:3231–44. [PubMed: 16854976]
- SPECTOR JA, GREENWALD JA, WARREN SM, BOULETREAU PJ, CRISERA FE, MEHRARA BJ, LONGAKER MT. Co-culture of osteoblasts with immature dural cells causes an increased rate and degree of osteoblast differentiation. *Plast Reconstr Surg.* 2002a; 109:631–42. discussion 643–4. [PubMed: 11818846]
- SPECTOR JA, GREENWALD JA, WARREN SM, BOULETREAU PJ, DETCH RC, FAGENHOLZ PJ, CRISERA FE, LONGAKER MT. Dura mater biology: autocrine and paracrine effects of fibroblast growth factor 2. *Plast Reconstr Surg.* 2002b; 109:645–54. [PubMed: 11818848]
- STRECKER S, FU Y, LIU Y, MAYE P. Generation and characterization of Osterix-Cherry reporter mice. *Genesis.* 2013; 51:246–58. [PubMed: 23180553]
- TABLER JM, BARRELL WB, SZABO-ROGERS HL, HEALY C, YEUNG Y, PERDIGUERO EG, SCHULZ C, YANNAKOUDAKIS BZ, MESBAHI A, WLODARCZYK B, GEISSMANN F, FINNELL RH, WALLINGFORD JB, LIU KJ. Fuz mutant mice reveal shared mechanisms between ciliopathies and FGF-related syndromes. *Dev Cell.* 2013; 25:623–35. [PubMed: 23806618]
- TOKUMARU AM, BARKOVICH AJ, CIRICILLO SF, EDWARDS MS. Skull base and calvarial deformities: association with intracranial changes in craniofacial syndromes. *AJNR Am J Neuroradiol.* 1996; 17:619–30. [PubMed: 8730180]
- TWIGG SR, WILKIE AO. New insights into craniofacial malformations. *Hum Mol Genet.* 2015; 24:R50–9. [PubMed: 26085576]
- YANNAKOUDAKIS BZ, LIU KJ. Common skeletal features in rare diseases: New links between ciliopathies and FGF-related syndromes. *Rare Dis.* 2013; 1:e27109. [PubMed: 25003013]
- YOSHIDA T, PHYLACTOU LA, UNEY JB, ISHIKAWA I, ETO K, ISEKI S. Twist is required for establishment of the mouse coronal suture. *J Anat.* 2005; 206:437–44. [PubMed: 15857364]
- YOSHIDA T, VIVATBUTSIRI P, MORRISS-KAY G, SAGA Y, ISEKI S. Cell lineage in mammalian craniofacial mesenchyme. *Mech Dev.* 2008; 125:797–808. [PubMed: 18617001]

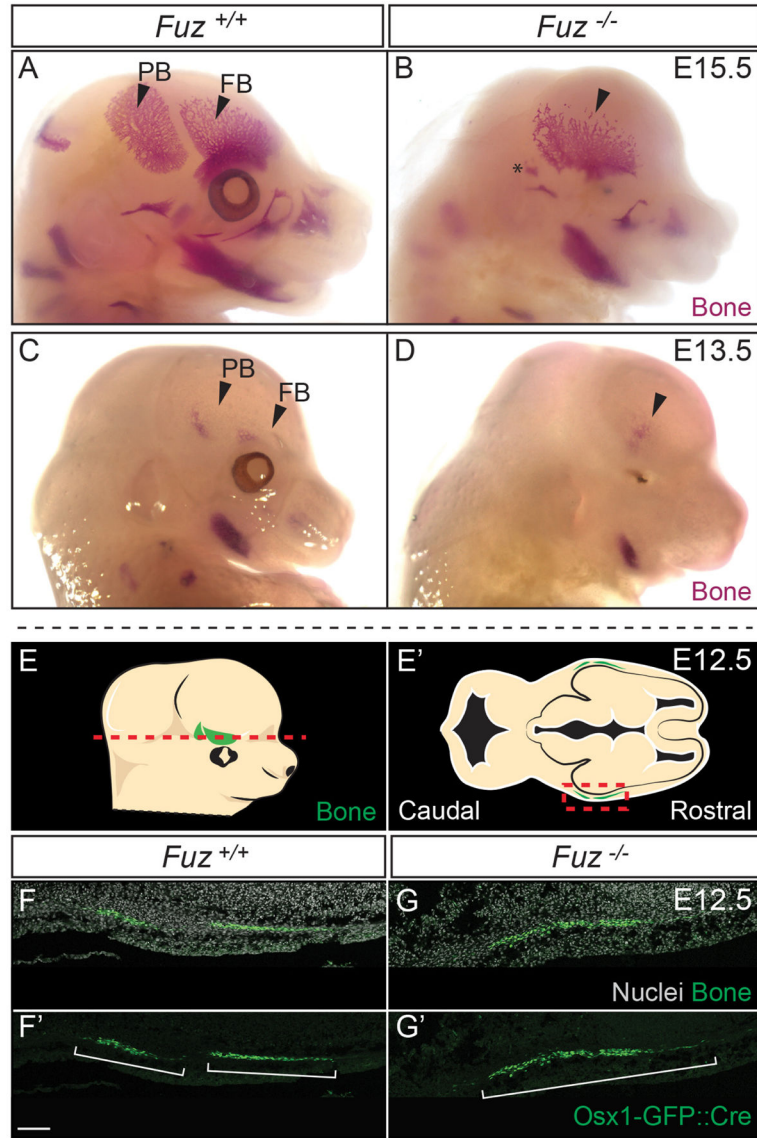


Figure 1. *Fuz* mutants form a single calvarial bone pair and no coronal suture
 (A–B) Alizarin red staining of E15.5 embryos. (A) *Fuz*^{+/+} embryo shows frontal (FB) and parietal bones (PB) separated by the coronal suture (CS) (n=5). (B) *Fuz*^{-/-} embryo showing a single bone plate (black arrowhead) (n=4). (C–D) Alizarin red staining of E13.5 embryos. (C) Two mineralization centers are observed in *Fuz*^{+/+} embryos (n=12). (D) *Fuz*^{-/-} embryo showing a single mineralization site (black arrowhead) (n=6). (E–E′) Schematics indicating sectional plane and anatomy represented in (G–J′). (F–G′) Horizontal sections of E12.5 embryos showing *Osx1*-GFP::Cre expression (green) and nuclei (grey). (F–F′) Two domains of GFP expression correspond to the frontal and parietal bones in *Fuz*^{+/+} embryos (n=4). (G–G′) A single GFP domain is observed in *Fuz* mutant (n=3).

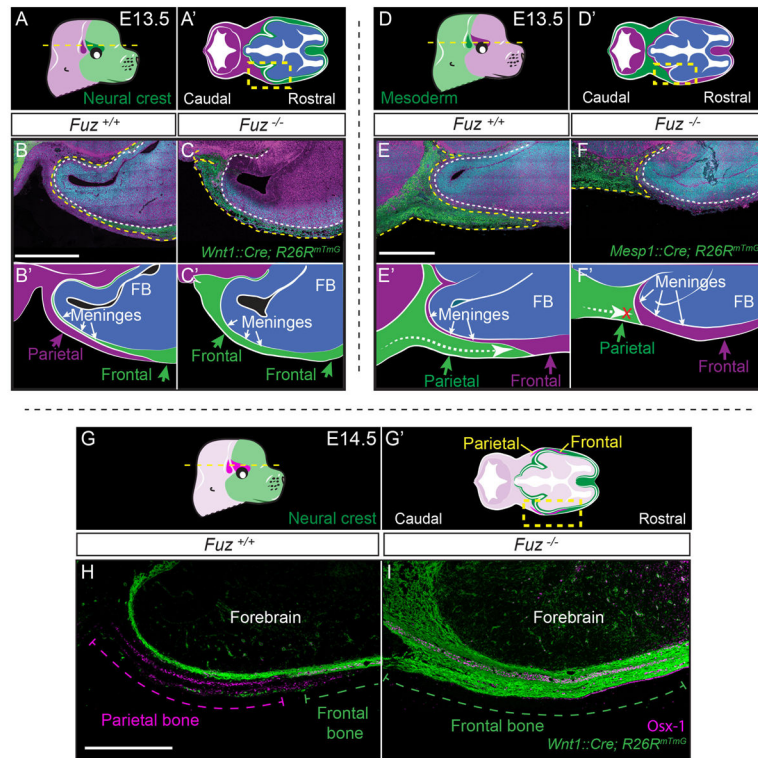


Figure 2. Single bone pair in *Fuz* mutants is neural crest-derived at the expense of parietal mesenchyme

(A–A′) Schematics indicating experimental design, sectional plane (yellow dotted line), and anatomy represented in B–F′. (B–C, E–F) Horizontal section of embryos where *Wnt1*Cre drives membrane GFP (green), all other tissues are labeled with membrane tdTomato (magenta), and nuclei are in cyan. Yellow dotted lines outline neural crest derivatives. White dotted lines outline forebrain. (B–B′) In wildtype E13.5 animals, GFP-labeled neural crest derivatives comprise frontal bone mesenchyme and meninges. (C–C′) Thick layer of GFP labeled frontal mesenchyme encases entire forebrain in E13.5 *Fuz*^{−/−} embryos (n=5). (D–D′) Schematics indicating experimental design, sectional plane (yellow dotted line), and anatomy represented in B–C′. (B–C, E–G) Horizontal section of embryos where *Mesp1*Cre drives membrane GFP (green), all other tissues are labeled with membrane tdTomato (magenta), and nuclei are in cyan. Yellow dotted lines outline mesoderm derivatives. White dotted lines outline forebrain. (E–E′) E13.5 *Fuz*^{+/+} embryo shows that GFP-labeled paraxial mesoderm overlies forebrain (n=5). (F–F′) E13.5 *Fuz*^{−/−} GFP-labeled mesoderm does not overlie forebrain (n=3). Scale bars indicate 500μm. (G–G′) Schematics indicating experimental design, sectional plane (yellow dotted line), and anatomy represented in (H–I). (H–I) Horizontal section of E14.5 embryos where *Wnt1*Cre drives membrane GFP (green) and *Osx1* positive osteoblasts are labeled in magenta, GFP-labeled neural crest derivatives comprise frontal bone mesenchyme and meninges. (H) *Osx1* positive, GFP negative cells comprise the parietal bone in WT mutants. (I) *Osx1* positive, GFP negative cells are absent in mutants. Scale bars indicate 500μm.

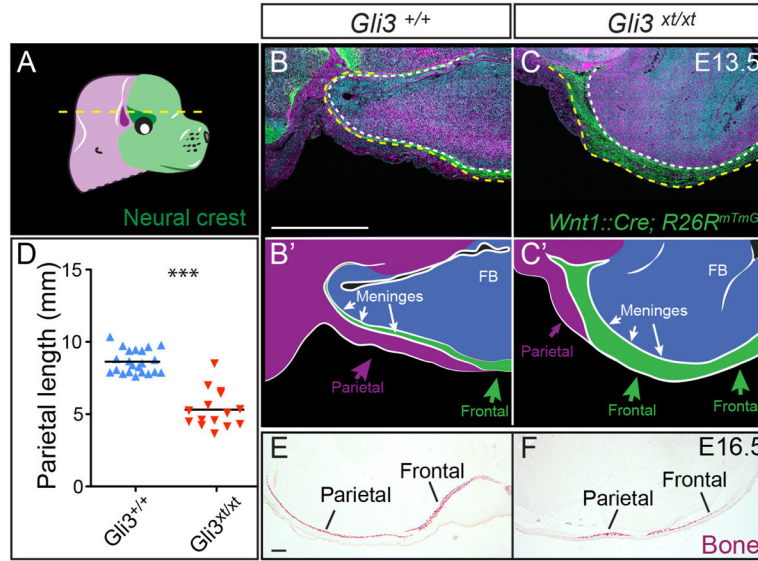


Figure 3. Loss of Gli3 is sufficient to expand neural crest-derived frontal mesenchyme at the expense of parietal mesenchyme
 (A–A') Schematics indicating experimental design, sectional plane (yellow dotted line), and anatomy represented in B–C'. (B–C) Horizontal section of embryos where Wnt1Cre drives membrane GFP (green), all other tissues are labeled with membrane tdTomato (magenta), and nuclei are in cyan. Yellow dotted lines outline neural crest derivatives. White dotted lines outline forebrain. (B–B') In wildtype E13.5 animals, GFP-labeled neural crest derivatives comprise frontal bone mesenchyme and meninges. (C–C') Increased frontal mesenchyme is observed E13.5 $Gli3^{xt-j/xt-j}$ embryos (n=3) compared to control embryos (B, n=5). Parietal mesenchymal lip that overlies forebrain (magenta, B and C) is decreased in mutant embryos. (D) Quantification of parietal bone length (mm) in three representative sections from each E16.5 $Gli3^{+/+}$ and $Gli3^{xt-j/xt-j}$ embryo (p=0.01). (E–F) Horizontal sections of E16.5 embryos stained with Alizarin red. Parietal bone length is decreased in $Gli3^{xt-j/xt-j}$ embryos (F, n=7) compared to $Gli3^{+/+}$ embryos (E, n=9). Scale bar indicate 100 μ m.

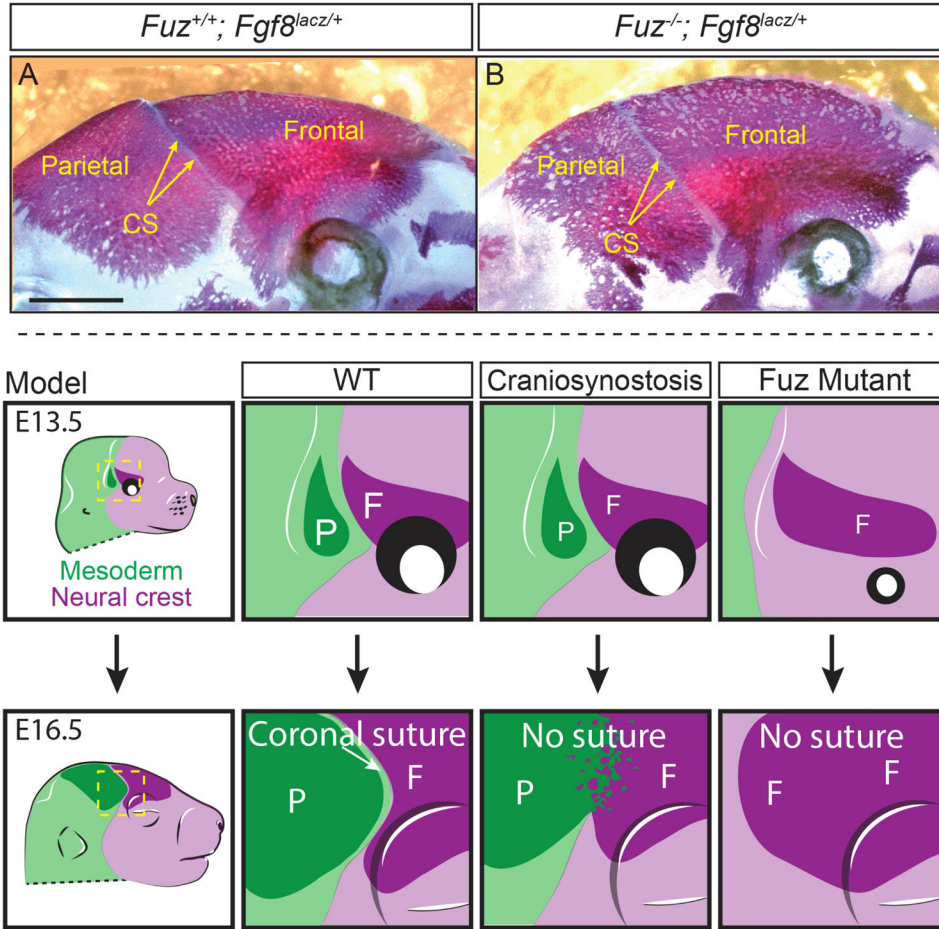


Figure 4. Genetic reduction of Fgf8 rescues parietal bone in Fuz mutants
 (A–B) Lateral view of alizarin red stained E17.5 embryos. (A) Frontal and parietal bones are separated by the coronal suture (CS) in $Fgf8^{lacz/+};Fuz^{+/+}$ control embryo. (B) Synostosis is rescued in $Fuz^{-/-};Fgf8^{lacz/+}$ embryo as frontal and parietal bones are separated by unossified coronal suture (CS). Scale bar indicates 1mm. **Model schematic.** The Fuz mutant skull phenotype is distinct from craniosynostosis.